Experimental Investigation of Three-Phase Low-Liquid-Loading Flow

Hamidreza Karami, Carlos F. Torres, Eduardo Pereyra, and **Cem Sarica,** University of Tulsa

Summary

An experimental study is conducted by use of a 6-in.-inner-diameter (ID) facility to investigate characteristics of three-phase stratified wavy flow in horizontal pipelines. The experiments are conducted under low-liquid-loading condition, which is very commonly observed in wet-gas pipelines. The analyzed flow characteristics include wave pattern, liquid holdup, water holdup, pressure gradient, and wetted-wall fraction.

The experimental range covers superficial-gas-velocity (v_{Sg}) values of 8 to 23 m/s, superficial-liquid-velocity (v_{SL}) values of 1 to 2 cm/s, and inlet-liquid-stream water-cut values of 0 to 100%. Differential-pressure transmitters, a quick-closing valve and pigging system, and a high-speed camera are used to acquire the data. The trends of the data with respect to input parameters are investigated. The performances of commonly used models are compared with liquid-holdup, pressure-gradient, and water-holdup experimental results.

The observed wave patterns include stratified smooth and stratified wavy with 2D waves, 3D waves, roll waves, and atomization flow. The transitions between the flow patterns vary as a function of water cut. The trends of pressure gradient, liquid holdup, and water holdup with respect to v_{Sg}, v_{SL}, and water cut are observed, and interpretations on the basis of physics are provided. The predictions of a transient multiphase-simulation software; the Tulsa University Fluid Flow Projects (TUFFP) unified model (Zhang et al. 2003), version 2012; Beggs and Brill (1973); Taitel and Dukler (1976); and Xiao et al. (1990) are compared with the acquired experimental data. The results from the transient multiphase-simulation software, Taitel and Dukler (1976), and Xiao et al. (1990) are in good agreement with experimental liquid-holdup and pressure-gradient data, but the three-phase water-holdup trends are not predicted well. The complicated nature of liquid/liquid interactions in three-phase low-liquid-loading flow causes greater uncertainties in predictions.

The number of experimental three-phase data, especially with larger pipe diameters, is very limited. This paper provides comprehensive data for three-phase stratified flow for a 6-in.-ID pipe. In addition, the prediction performance of the commonly used predictive tools in the industry is provided.

Introduction

Low-liquid-loading flow is a flow condition wherein the liquid-flow rate is very small compared with the gas-flow rate. It is widely encountered in wet-gas and gas/condensate pipelines. Even though the pipeline is fed with single-phase gas, the condensation of the heavier components of the gas phase, along with traces of water, results in three-phase flow. The presence of these liquids in the pipeline, although in very small amounts, can significantly influence flow characteristics such as pressure gradient and liquid holdup. Therefore, understanding of the flow characteristics of low-liquid-loading gas/oil/water flow is of great importance in transportation of wet gases.

This paper (SPE 174926) was accepted for presentation at the SPE Annual Technical Conference and Exhibition, Houston, 28–30 September 2015, and revised for publication. Original manuscript received for review 29 October 2015. Paper peer approved 4 January 2016.

Although many different studies have been conducted on gas/liquid multiphase flow, only a very small number of three-phase flow studies, especially for low-liquid-loading flows, can be found. These studies are mainly experimental, and focused on two-phase flow in small-diameter pipelines. The coexistence of thin films of water along with oil in production systems is very commonly observed in wet-gas pipelines. The existence of the second liquid phase influences all of the flow characteristics. The three-phase-flow behavior can be considered as a combination of gas/liquid and oil/aqueous phase interactions.

Meng et al. (2001) conducted two-phase-flow experiments for oil/air flow in a 2-in.-ID pipe. They observed a surprising decrease in liquid holdup and pressure gradient when the v_{SL} was increased. They attributed this decrease to the increase in droplet entrainment. They also developed a correlation for interfacial friction factor.

Fan (2005) used two experimental facilities with IDs of 2 and 6 in., respectively, to conduct two-phase water/air low-liquid-loading experiments. Fan observed stratified smooth and stratified wavy flow patterns in his experiments with the 6-in.-ID facility. With the 2-in.-ID facility, in addition to stratified flow patterns, an annular flow pattern was observed. Fan used the acquired experimental data to develop new closure relationships for mechanistic modeling. These closure relationships included wetted-wall fraction, liquid-wall friction factor, and interfacial friction factor.

Later, Dong (2007) modified the 6-in.-ID facility of Fan (2005) to conduct low-liquid-loading three-phase-flow experiments. Water, air, and oil with a viscosity of 13 cp were the flowing fluids. This is a relatively high oil viscosity compared with the commonly observed values in wet-gas pipelines, and the results may not be representative for wet-gas pipeline systems. The distribution of oil and water in liquid phase for different flowing conditions was observed and categorized. In addition, a model comparison was provided for flow characteristics.

Recently, Gawas (2013) used the same 6-in.-ID facility of Dong (2007) to investigate the characteristics of three-phase low-liquid-loading flow. Gawas conducted his experiments by use of an oil with a viscosity of 1.3 cp for different values of water cut, and developed correlations for entrainment of liquid droplets in gas phase for two- and three-phase flows. He also analyzed the droplet-size distribution and developed a correlation for interfacial wave celerity. In addition, several studies have been conducted in other research centers to analyze low-liquid-loading flow. A summary of these studies is presented in Gawas (2013).

In the current study, the facility of Gawas (2013) is used. The main objective of this research is to study low-liquid-loading three-phase flow, and the targeted flow parameters are liquid holdup, water holdup, wave pattern, and pressure gradient. The experimental results for different flow characteristics are analyzed and evaluated to improve understanding of the flow phenomena. In addition, the commonly used models are evaluated by use of the acquired experimental data.

Experimental Design

In this study, experiments are conducted in a 6-in.-ID three-phase-flow loop. The flow loop consists of two parallel sections, with 6-in. (0.1524-m) -ID pipes. Each section is 56.4 m long. Acrylic vi-

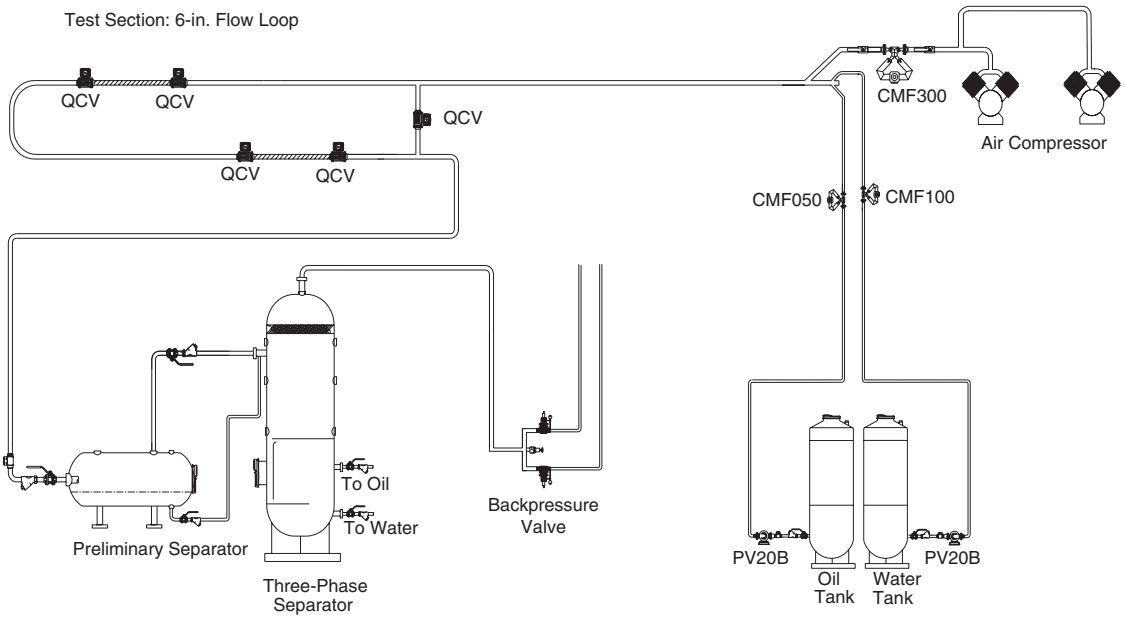

Fig. 1—6-in.-ID low-liquid-loading facility.

sualization sections, approximately 8 m long, are provided at the end of each section. These visualization sections are located where all the measurement systems are installed, providing sufficient length for flow development. Two backpressure valves were installed at the outlet of the separator to control the pressure in the flow loop. The pressure in the flow loop is kept constant at approximately 9 psig for all of the experiments to avoid significant changes in fluid characteristics.

Water and oil are kept in separate tanks, each having a capacity of 500 gal. They are pumped from their respective tanks by use of progressing cavity pumps with maximum pumping capacity of 11.5 gal/min. Air is supplied through two different compressors, with combined capacity of 2,640 scf/min at a compressor outlet pressure of 100 psig (Gawas 2013). After flowing through the test section, the fluids are separated by use of two separators (horizontal and vertical). This helps minimize the trapped droplets flowing in the gas phase. Separated air is vented to the atmosphere, and oil and water are circulated back to their tanks.

Air-, oil-, and water-flow rates are measured by use of Coriolis-type mass flowmeters (CMF300, CMF050, and CMF100, respectively) before the mixing tee. This facility has been used previously to investigate two- and three-phase low-liquid-loading flow by several researchers, including Fan (2005), Dong (2007), and Gawas (2013). **Fig. 1** shows a schematic of the facility.

The operating fluids consist of compressed air as the gas phase, Isopar L as the oil phase, and tapwater as the aqueous phase. Because of the low-pressure condition and minor variations of the operating pressure in the test section, the viscosity of the gas phase was assumed to be constant during a particular test. Density of the gas phase was calculated at the operating pressure and temperature by use of the ideal-gas law. A tensiometer was used to verify the values of surface and interfacial tension for different liquid phases. This device has a reading accuracy of 1 dynes/cm and an uncertainty of ±2 dynes/cm. The interfacial-tension measurement of the oil/water interface was 37 dynes/cm. **Table 1** provides a summary of different fluid properties under operating conditions.

Fig. 2 shows a schematic of the test section for a low-liquid-loading facility. Pressure and temperature readings are taken at the indicated points in the test section with the installed pressure and temperature transducers. In addition, three differential-pressure

Fluid	ρ (kg/m^3)	μ (cp)	σ (dynes/cm)
Air	1.9	0.018	NA
Isopar L oil	760	1.27	24
Tap water	995	0.9	68

Table 1—Fluid properties for different phases in operating conditions.

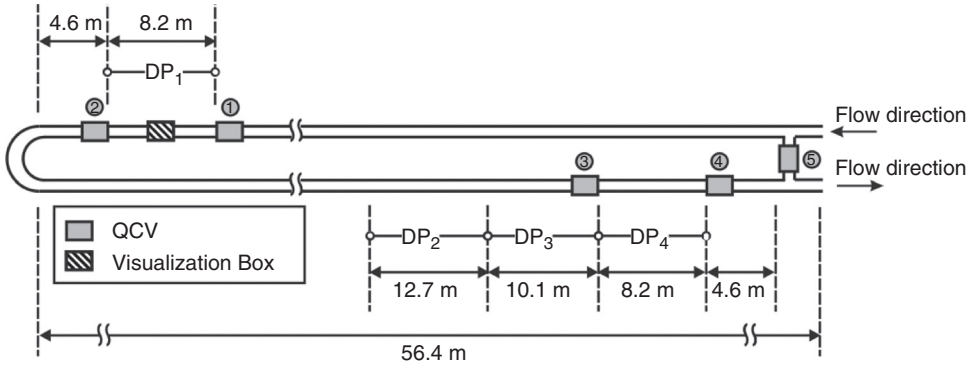

Fig. 2—Test-section schematic for low-liquid-loading facility.

Fig. 3—Picture of QCVs and schematic of pigging system.

transmitters are installed at each run of the test section providing pressure difference between the two ends of the transmitter-impulse lines. The four transmitters that were used in this work are shown in Fig. 2.

Averaging the differential-pressure-transmitter readings provides a good estimate of the pressure gradient in the test section. The probes are connected to the top of the test section to ensure that impulse lines are filled with air. The uncertainty of the differential-pressure transmitters is estimated at 0.17 in. of H_2O by the manufacturer. Considering random sources of uncertainty, this value is considered to be 0.20 in. of H_2O. To obtain the dynamic wetted-wall-fraction (DWWF) measurements, four different scales were placed on the outer pipe periphery in the visualization boxes. The readings were divided by the total pipe periphery to get the wetted-wall fraction.

Five quick-closing valves (QCVs), as shown in Fig. 2, are used to trap the liquid in the test sections and bypass the flow. **Fig. 3** shows a picture of one set of fluid-trapping QCVs and a schematic of the pigging system.

The reaction time of the QCV (knife type) is less than 1 second. The liquid trapped between QCVs is pigged out with a specially designed pigging system, and is drained into graduated cylinders to measure the oil and water volumes. The liquid holdup was calculated by dividing the collected liquid volume by the volume of the test section. The pigging-efficiency tests were carried out using oil and water as the liquid phase to determine the uncertainties. It was realized that approximately 96% of the liquid is drained after first pigging, and this number increases to more than 98% after second pigging. It was decided to carry out two pigging operations for each liquid-holdup measurement and add 100 mL (≈0.05% of total section volume) to the experimental readings to account for the residual liquid in the test section.

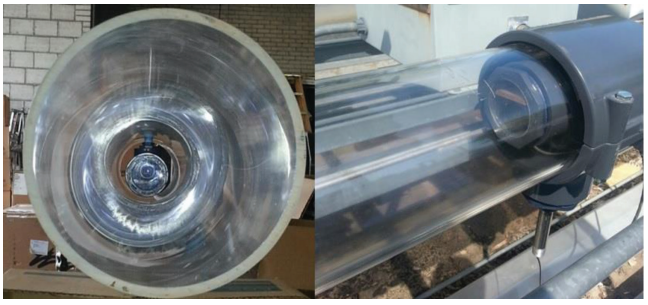

Fig. 4—Visualization camera and its position inside the test section.

A small-sized camera was placed in the test section to visualize the wave patterns and estimate the onset of droplet entrainment. The camera had an iris lens system, and was connected and charged through an ethernet connection. This helped optimize the design because only one connecting cable was required inside the test section. The camera was positioned concentrically inside the pipe, and the focal point was 10 in. upstream of the camera. Gas-flow rates are high enough to avoid deviation of the flow streamlines because of the intrusive nature of the camera at this focal point. **Fig. 4** shows a picture of the camera and its position inside the test section.

The video-capturing speed was set at 100 frames/second, recording videos with a speed approximately 2.5 times faster than the actual fluid velocity. For different values of v_{SL}, v_{Sg} was increased in a step-by-step fashion, and videos of the interfacial wave structure were recorded. This was continued until the point at which significant droplet entrainment made the pictures blurry. The resulting videos provided a clear picture of wave-pattern transitions and onset of entrainment.

Experimental Results

In this section, the experimental results for different flow characteristics are discussed and evaluated. All of the tests were conducted in horizontal configuration and with stratified wavy flow pattern. Water-cut values were varied from 0 to 100%, and v_{SL} values of 1 and 2 cm/s and v_{Sg} values of 8 to 23 m/s were studied.

Pressure Gradient. The single-phase air-flow readings were compared with Colebrook's equation predictions to validate pressure-gradient readings in **Fig. 5.** Using the pipe roughness value of 10^{-4} m, the equation results matched the pressure-gradient readings, providing more confidence about the readings. This relatively higher roughness can be a result of effects of pipe joints and aged pipes. **Fig. 6** shows the two-phase and three-phase pressure-gradient results for different water-cut values. Data with v_{SL} values of 1 and 2 cm/s are included in the plot. Single-phase air-flow data are added for comparison purposes. As expected, pressure gradient of multiphase low-liquid-loading flow is mainly influenced by the gas-flow rate. There is a slight change in pressure gradient for two different v_{SL} values. However, the increase with higher v_{Sg} values is much more pronounced. This can be explained through the thin film of liquid and strong influence of interfacial waves and drag force applied by gas phase to carry the liquid. Water cut does not seem to make an appreciable impact. However, two-phase oil/air flow gives

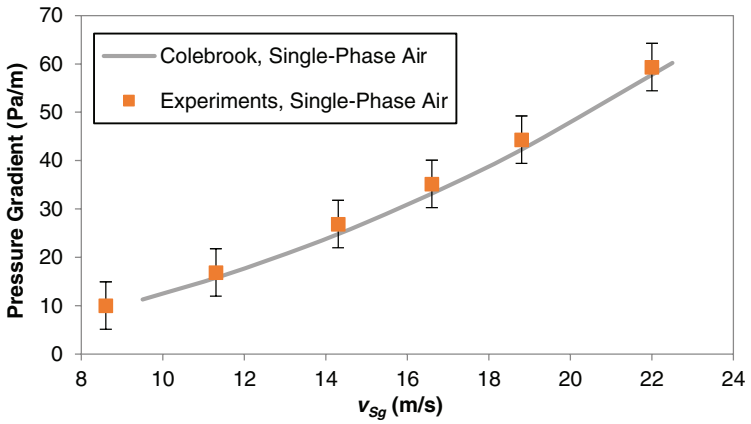

Fig. 5—Verification of pressure-gradient data with Colebrook's equation.

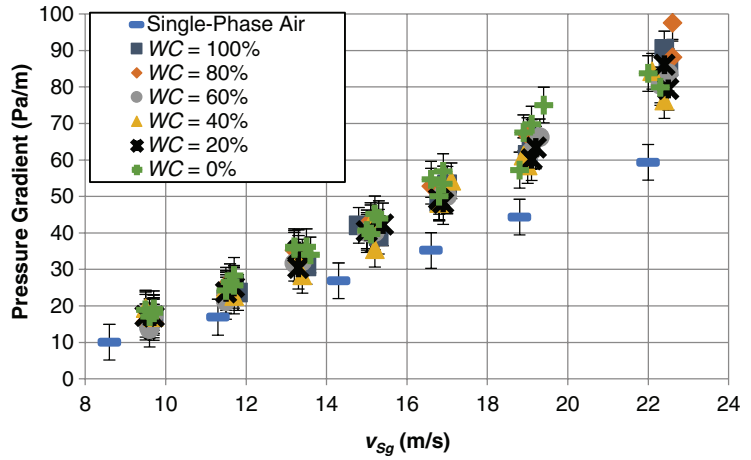

Fig. 6—Three-phase pressure-gradient data with different water cuts.

a slightly higher pressure gradient compared with other water-cut cases. This can be because of a slight decrease in liquid holdup for the oil/air case, primarily owing to the lower density of the oil.

Liquid Holdup. **Fig. 7** shows the two-phase and three-phase liquid-holdup results with different water-cut values for a v_{SL} value of 2 cm/s. It was observed that increasing v_{SL} from 1 to 2 cm/s results in an increase in the liquid holdup. However, the data follow the same trend for the case in which the v_{SL} value is 1 cm/s.

One can see that liquid holdup decreases with increasing v_{Sg}. This is because of stronger wave structure and interfacial shear stress, and resulting increase in the liquid-phase velocity. Oil and

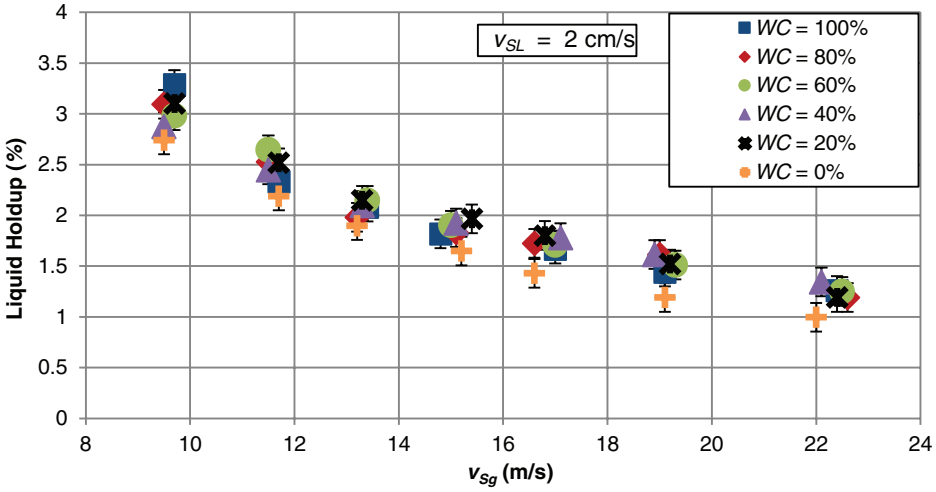

Fig. 7—Three-phase liquid-holdup data with different water cuts.

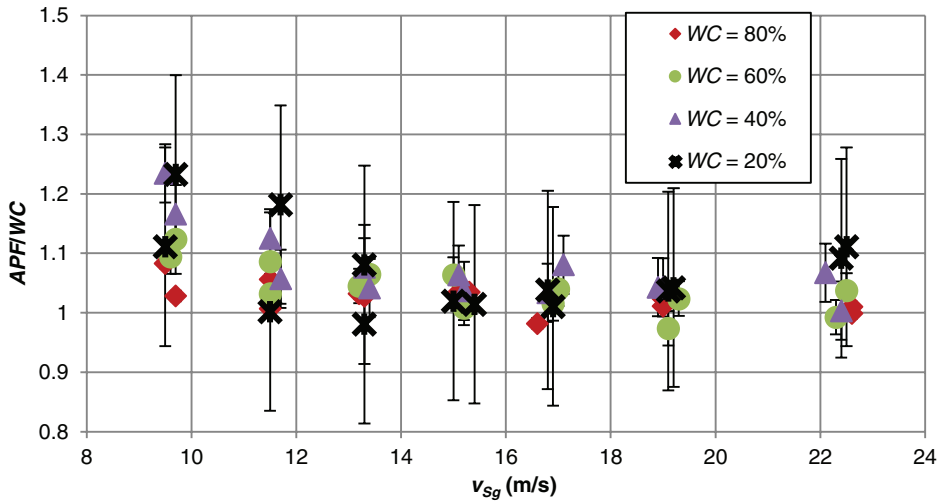

Fig. 8—Three-phase aqueous-phase-fraction data with given water cuts.

water phases have relatively similar physical properties. Consequently, the results are not noticeably affected by water cut. However, the tests with water cut of 0% (oil/air) produce slightly lower liquid-holdup values. Lower oil density causing stronger wave structure for a constant interfacial shear can be the reason for this minor decrease in liquid holdup compared with three-phase cases.

In addition to the liquid volume, the volume of aqueous phase was measured for three-phase-flow cases to estimate the fraction of aqueous phase in flowing stream (*APF*). Comparing this value with that of the inlet-stream water cut gives an estimate of slippage in the liquid phase. *APF* should be equal to water cut for a homogeneous oil and aqueous-phase mixture. However, primarily, the density difference between the phases can cause water and oil segregation. On the other hand, layers of liquid phase closer to the gas interface have significantly higher velocities than layers closer to the wall. This vertical velocity profile, along with full or partial separation of oil and aqueous phases, causes some slippage between the liquid phases.

Fig. 8 shows the three-phase relative aqueous-phase-fraction results for various water cuts. Data with v_{SL} values of 1 and 2 cm/s are included in the plot. The vertical axis shows the ratio of *APF* and water cut. This value should be equal to unity for a homogeneous liquid mixture. However, it is higher than unity for most cases. In the lower-gas-flow-rate region, up to v_{Sg} values of 18 to 19 m/s, aqueous-phase fraction decreases and the plotted ratio becomes closer to unity by increasing the v_{Sg} value. It reaches close to unity for the v_{Sg} range of 15 to 18 m/s. This can be because of the relative increase in the strength of turbulent mixing forces in comparison to gravitational segregation and surface forces. In higher v_{Sg} range, a slight increase is observed in aqueous-phase-fraction values, possibly resulting from higher entrainment of the oil phase compared with the aqueous phase. Gawas (2013) and Karami (2015) presented the entrainment fraction data for three-phase low-liquid-loading flow and observed significantly higher entrainment fraction values for oil droplets compared with water droplets at the same v_{Sg} range.

DWWF. DWWF is defined as the fraction of the inner pipe wall that is wetted by a continuous liquid-film flow. Different phenomena, such as change in liquid holdup, droplet entrainment, and curvature of interface because of surface forces, can affect the estimated DWWF value. **Fig. 9** shows the DWWF results for various water cuts and v_{SL} values of 1 and 2 cm/s. The trends are very similar for the two v_{SL} values. No clear trend is observed with v_{Sg}, and data are scattered in the DWWF range of 0.1 to 0.2. Apparently, different effects, such as liquid-holdup decrease, entrainment-rate increase, and changing of the interface shape, are cancelling each other, and a clear trend could not be observed.

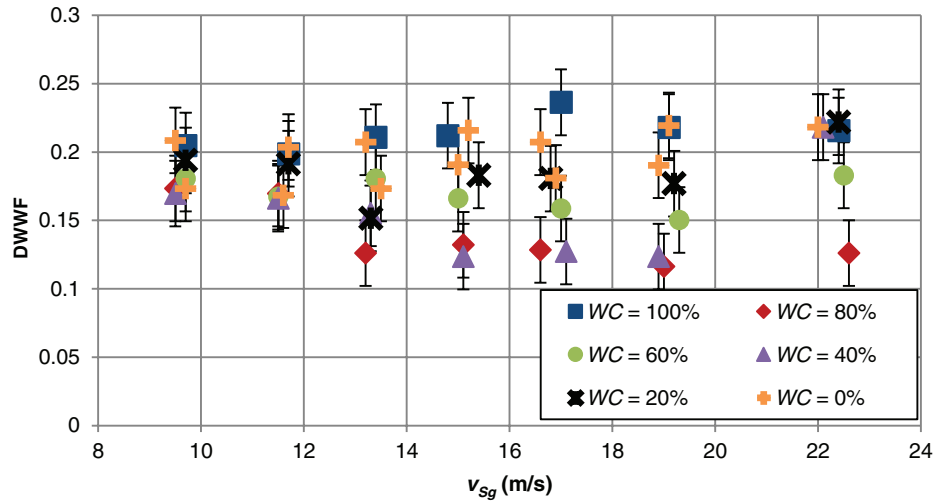

Fig. 9—Three-phase wetted-wall-fraction data for various water cuts.

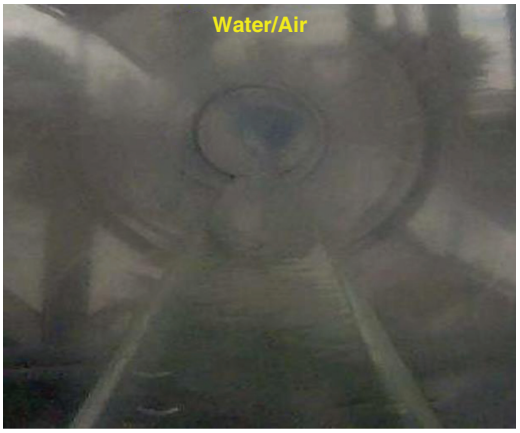

Fig. 10—Stratified, smooth-flow-pattern picture for water/air flow.

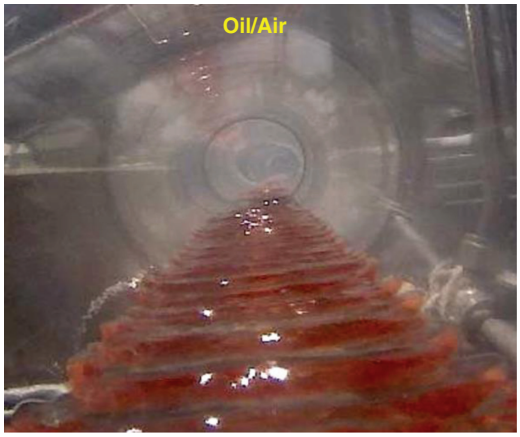

Fig. 11—Stratified wavy flow pattern with 2D wave structure for oil/air flow.

Visual Observations of Waves and Atomization. The appearance of first instabilities or waves at the gas/liquid interface is considered as the transition from stratified smooth to stratified wavy flow. However, the wave structures change with the flowing conditions. The 2D wave structure is the first wave regime appearing at the interface. By increasing gas-flow rate, the 2D waves are replaced by 3D waves, and then by more-irregular roll waves. If the gas-flow rate is increased further, atomization of liquid droplets starts.

The experiments were conducted for v_{SL} values of 1 and 2 cm/s. Experiments were started with the lowest operating v_{Sg} value of 4 m/s, and it was raised in steps of 0.5 or 1 m/s. The point at which the entrained droplets reach the center of the pipeline and hit the protective glass in front of the camera is considered to be the onset of atomization. Shortly after this point, droplet entrainment becomes much more significant and makes the test section blurry, prohibiting further investigation of wave structure for higher gas-flow rates.

The first flow pattern observed for very low gas-flow rates is stratified smooth flow. This flow pattern was observed for the cases with water at very low v_{Sg} values up to approximately 5 m/s. However, for the case with oil as the liquid phase, the observed flow pattern was always stratified wavy for the v_{Sg} range of this study. **Fig. 10** shows the stratified smooth flow with water as the liquid phase for v_{Sg} value of 4 m/s and v_{SL} value of 1 cm/s. No wave structure is observed at these cases, and the interface is very stable.

After transition to stratified wavy flow pattern, the first wave regime is 2D waves. The 2D waves are extended at the interface across the pipe cross section, and include interface movements and liquid-level fluctuations only in the vertical direction. **Fig. 11** shows the 2D wave structure for the case with oil as the liquid phase. The v_{Sg} value is 3 m/s, and the v_{SL} value is 1 cm/s. This regime does not cover a wide range of gas-flow rates, and gives place to 3D waves by increasing v_{Sg} by only 1 m/s for all cases. For the oil case, capillary waves appear at the liquid/wall boundary and the wetted-wall fraction fluctuates. However, for the water case, possibly because of higher surface resistance, no 2D wave structure was observed.

Increasing the v_{Sg} causes a transition from 2D waves to 3D waves. The wave lengths become shorter and the interface structure becomes much more complex. The waves still have a regular shape; however, the front of the wave is curved and positioned more torward the center as compared with the points closer to the wall. **Fig. 12** shows the pictures of 3D wave structure for the cases with oil and water as the liquid phase. The v_{Sg} value is 4 m/s for the oil case and 6 m/s for the water case. Tangential capillary waves are noticeable for oil/air flow, but are not as significant for water/air flow. Lower surface tension of oil can be the reason for stronger capillary waves. The wave amplitude seems to be higher for the oil case, and the lower density of the oil phase makes the wave structure stronger for a given interfacial shear stress.

While in the 3D wave regime, further increases in gas-flow rate increase the irregularities in the wave shape, and cause a gradual transition to a roll-wave regime. Roll waves are shock-like disturbances developing at the turbulent gas/liquid interface. Roll-wave structure is the most-dominant regime in stratified wavy flow pattern. **Fig. 13** shows pictures of small- and large-amplitude roll-wave structures for the cases with oil and water as the liquid phase. The

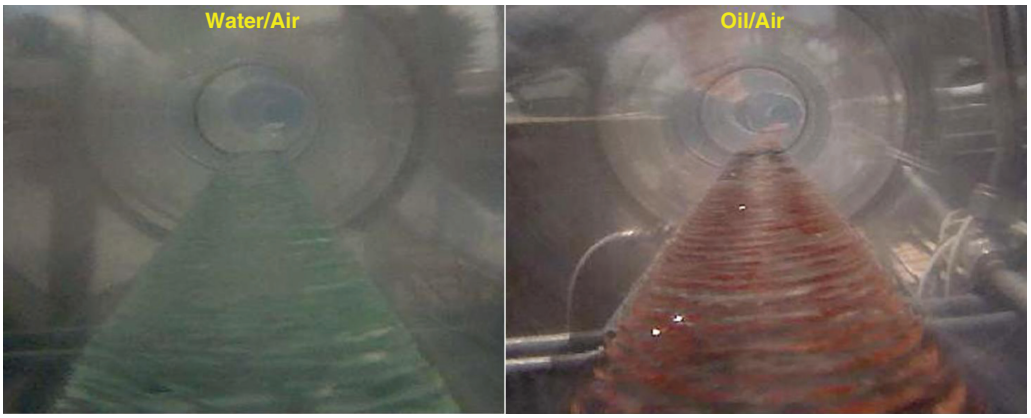

Fig. 12—Stratified wavy flow pattern with 3D wave structure for water/air and oil/air flow.

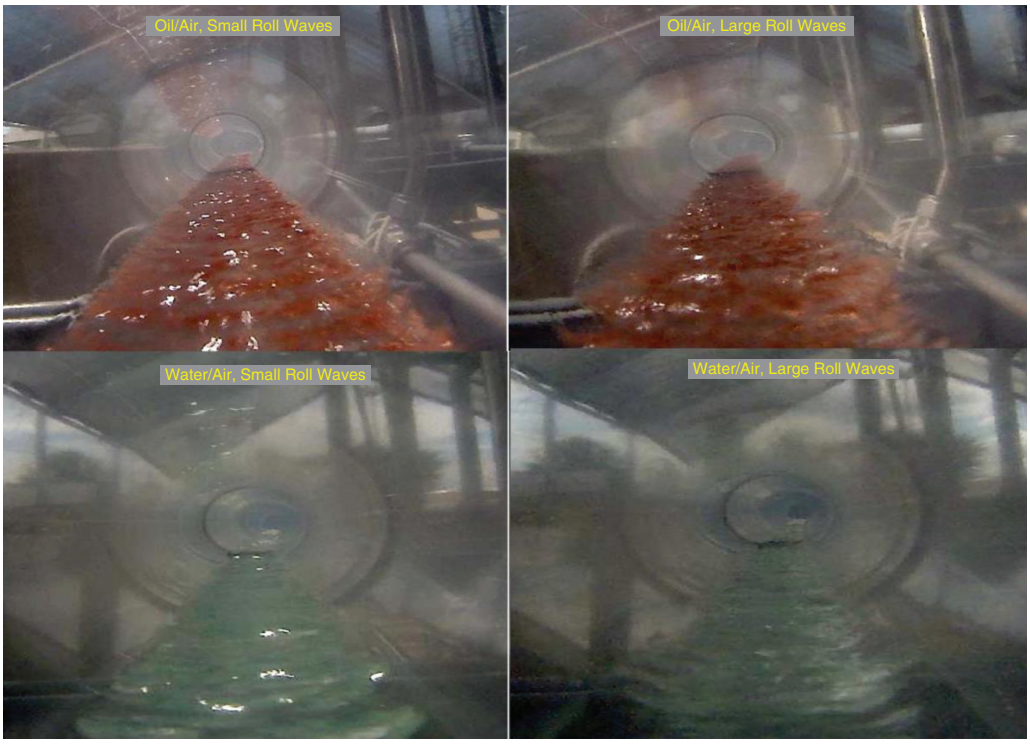

Fig. 13—Stratified wavy flow pattern with roll wave structure for water/air and oil/air flow.

v_{Sg} value for smaller-amplitude roll-wave structure is 6 m/s for the oil case and 8 m/s for the water case. The v_{Sg} values are 3 m/s greater for the case of larger-amplitude roll waves. Going from the lower to higher v_{Sg} values, the amplitude of roll waves increases significantly. This is a result of the higher interfacial shear stress applied by the gas phase. On the other hand, the tangential waves next to the side walls become more pronounced and the fluctuations in the wetted-wall level increase. This is again a result of the higher interfacial shear stress values and possibly secondary flows in the gas phase.

The onset of atomization occurs in the roll-wave regime. Once the amplitude of roll waves becomes strong enough, the gas stream is able to break the liquid section at the top of the wave and create liquid droplets flowing with the gas phase. **Fig. 14** shows pictures of the test section after the onset of atomization with oil and water as the liquid phase. Because the protective glass is oil-wet, the oil droplets spread on it, and it becomes harder to notice them in the picture. The v_{Sg} values are 12 m/s for water and 10 m/s for the oil case. For all cases, further increase in the v_{Sg} value results in blurry pictures.

Fig. 15 shows the summary of transitions between the described wave regimes for two-phase flows with oil or water as the liquid phase. All the transitions are occurring at a lower v_{Sg} value for the oil case. As mentioned, this is because of the lower surface and gravitational forces in the liquid phase lowering the resistance to the gas-phase drag force. On the other hand, changing v_{SL} from 1 cm/s (shown by dashed lines) to 2 cm/s (shown by solid lines) does not make a substantial impact on the transitions in wave regimes. However, for higher liquid-flow rates, most of the transitions are occurring at a slightly lower v_{Sg} value.

Model Evaluation

The acquired experimental data were used to benchmark the performances of the existing models. The model comparisons were made

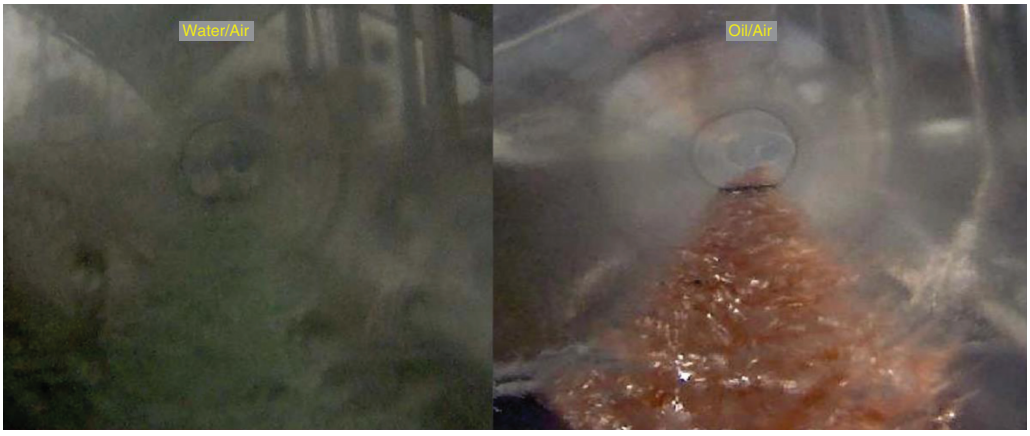

Fig. 14—Stratified wavy flow onset of atomization for water/air and oil/air flow.

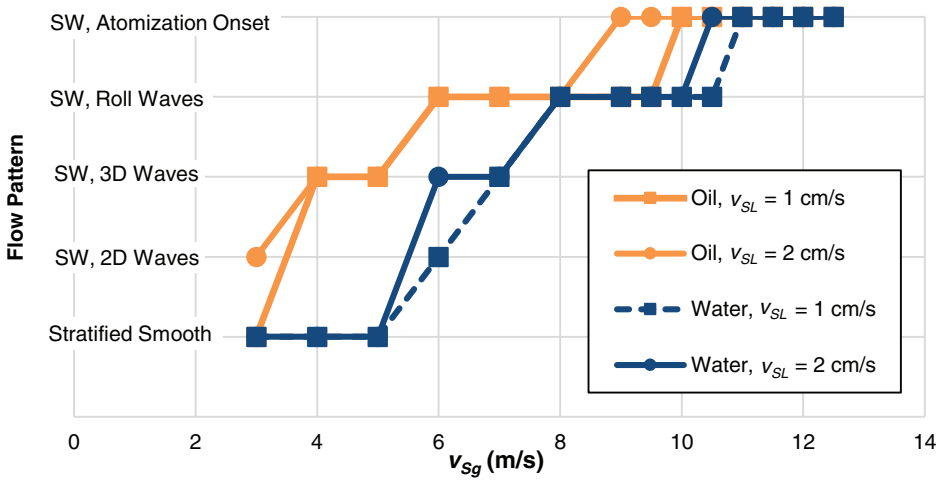

Fig. 15—Stratified flow-pattern transitions with v_{Sg} for water/air and oil/air flow.

for the cases of two- and three-phase flows with various water cuts for flow characteristics, including liquid holdup, pressure gradient, aqueous-phase fraction, and wave pattern.

Wave-Pattern Transitions. Andritsos and Hanratty (1987) suggested a model for wave-pattern transitions in stratified wavy flow. **Fig. 16** shows a comparison of the predictions from the Andritsos and Hanratty (1987) model with the acquired experimental data for wave-pattern transitions.

They adopted the onset of interface instabilities given by Taitel and Dukler (1976) as the transition to 2D waves. They used the v_{Sg} value at which Kelvin-Helmholtz instabilities appear as the onset of roll waves. Their recommended droplet-atomization superficial-gas-velocity ($v_{Sg,atom}$) value was 1.8 times the v_{Sg} value for the onset of roll waves. The data include the cases with oil or water as the liquid phase. The model seems to slightly underpredict the v_{Sg} values of transition for almost all cases, especially for the transition to 2D waves. However, the predictions are within an acceptable agreement with the observed data for transition to roll wave and atomization onset.

Two-Phase-Flow Prediction Evaluation. Transient multiphase-simulation software is one of the most common simulation tools in flow assurance. The software used in this study is based on a two-fluid model in which flow patterns are treated as integral parts of a two-fluid system. The basis of this simulation software is given in Bendiksen et al. (1991). The results are obtained with the Multiphase Toolkit of the software. In addition, the TUFFP unified model version 2012 is used to predict the values of different flow parameters for the conducted experiments. A comparison is made between the predicted and experimental values of liquid holdup and pressure gradient. The results from three other two-phase-flow models—namely, Taitel and Dukler (1976), Xiao et al. (1990), and Beggs and Brill (1973)—are also included in this model comparison.

Figs. 17 and 18 show the comparison of available experimental data for two-phase flow with the mentioned predictive tools for pressure gradient and liquid holdup, respectively. The Beggs and Brill (1973) correlation performs poorly for low-liquid-loading conditions. The pressure gradient is overpredicted, and the liquid holdup is significantly underpredicted. The Taitel and Dukler (1976) model, with the assumption of flat interface and f_I value of 0.0142, performs relatively better in predicting pressure gradient and liquid holdup. However, the discrepancies increase for higher-liquid-holdup-value data points. The Xiao et al. (1990) model, in essence, is the Taitel and Dukler (1976) model with a new interfacial friction factor, f_I.

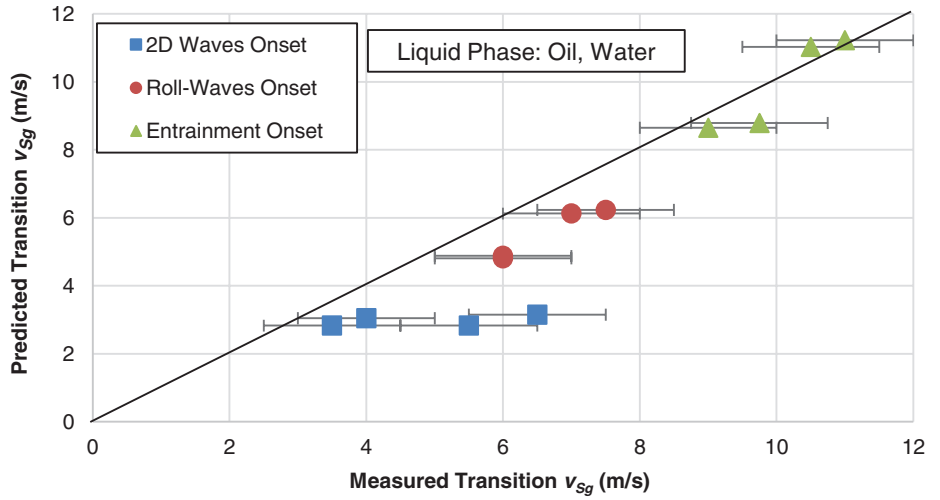

Fig. 16—Comparison of Andritsos and Hanratty (1987) wave-pattern transitions with experimental data.

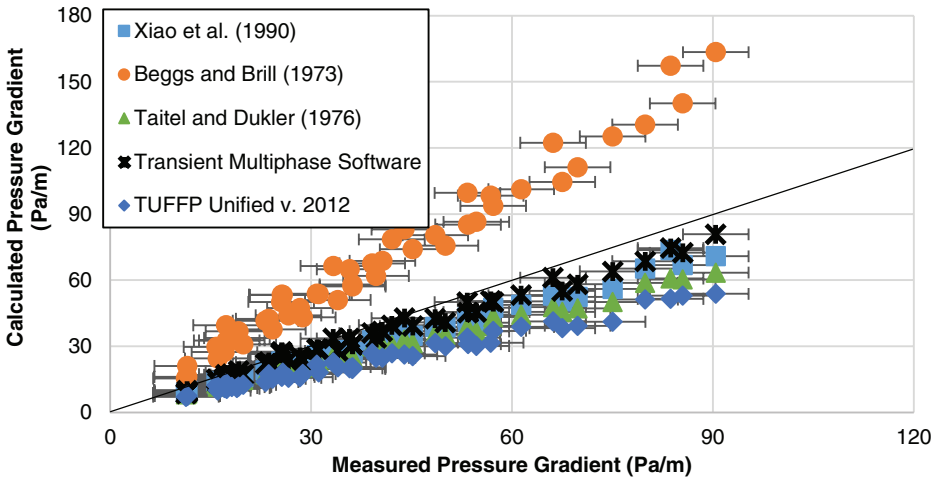

Fig. 17—Pressure-gradient data comparison with five common predictive tools.

Therefore, the predictions of this model are very close to Taitel and Dukler (1976) predictions. However, the new f_I definition seems to have slightly improved the model predictions.

Predictions from the transient multiphase-simulation software are in good agreement with experimental results. However, a minor overprediction of liquid holdup and underprediction of pressure gradient are observed. Definitions of different terms, such as interfacial friction factor, can cause this minor discrepancy. The TUFFP unified model version 2012 underpredicts the liquid holdup for all cases, especially for the cases with lower gas-flow rate corresponding to higher liquid-holdup data points. Pressure gradient is also underpredicted, especially for higher gas-flow rates corresponding to higher pressure-gradient values. The selection of closure relationships for various flow parameters under low-liquid-loading conditions has to be implemented with caution, and can be a potential source of errors in calculation procedure.

It can be observed that a flat-interface approach gives a good estimation of different flow characteristics when applied with Taitel and Dukler (1976) or similar models. Of course, this conclusion is valid only for the tests conducted with larger pipe diameters, where surface forces are relatively negligible. It can also be seen that an improved f_I closure relationship can have a noticeable impact on model predictions.

Table 2 shows the summary of a statistical analysis of pressure gradient and liquid-holdup predictions in comparison with the experimental data for the investigated models. The error terms defined by Xiao et al. (1990) are used. The terms ε_1, ε_2, and ε_3 are relative error terms, called average percent error, absolute average percent error, and percent standard deviation, respectively. The terms ε_4, ε_5, and ε_6 are absolute error terms, called average error, absolute average error, and standard deviation, respectively. The equations for these terms can be found in Xiao et al. (1990). The bottom row in Table 2 shows an estimate of the overall error (e_{Overall}) for each model. Eq. 1 gives the definition of this overall error term:

$$e_{\text{Overall}} = \sum_{i=1}^{3} \varepsilon_{i,H_L} + \sum_{i=1}^{3} \varepsilon_{i,PG} + 100 \times \left(\frac{\sum_{i=4}^{6} \varepsilon_{i,H_L}}{H_{L,\max}} + \frac{\sum_{i=4}^{6} \varepsilon_{i,PG}}{PG_{\max}} \right). \quad \text{.....(1)}$$

The transient multiphase-simulation software performs the best for pressure-gradient predictions. However, the best overall performance is by the stratified flow models of Taitel and Dukler (1976) and Xiao et al. (1990). This can be explained by the fact that these models are developed for stratified flow conditions with flat-interface geometry, which is more suitable for larger pipeline diameter with low-liquid-loading data points.

Three-Phase Flow-Prediction Evaluation. The predictions of the transient multiphase simulation software and TUFFP unified model

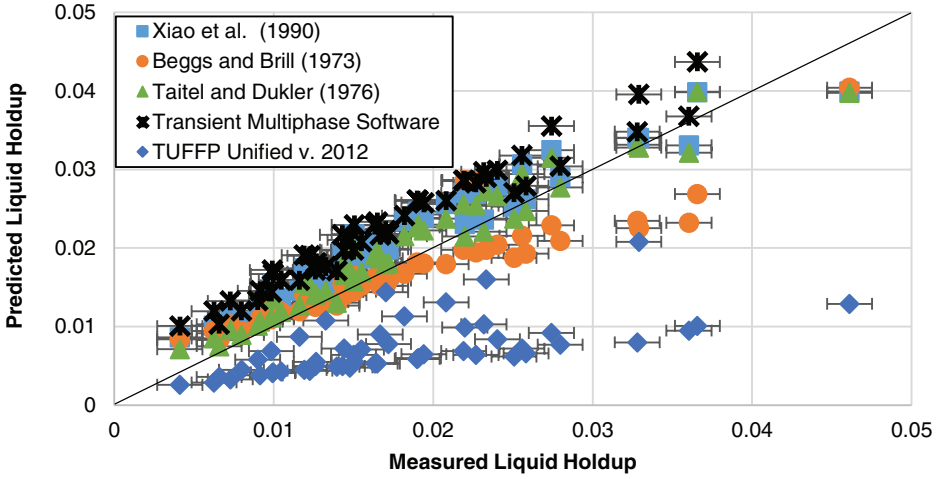

Fig. 18—Liquid-holdup data comparison with five common predictive tools.

Errors	Beggs and Brill (1973)	Xiao et al. (1990)	Taitel and Dukler (1976)	Transient Multiphase Software	TUFFP Unified Version 2012
Pressure gradient					
ε_1 (%)	72.17	–19.20	–26.24	–10.31	–37.83
ε_2 (%)	72.17	19.20	26.24	10.93	37.83
ε_3 (%)	104.38	25.18	23.79	37.65	27.31
ε_4 (Pa/m)	28.01	–7.87	–10.83	–4.39	–15.27
ε_5 (Pa/m)	28.01	7.87	10.83	4.55	15.27
ε_6 (Pa/m)	86.73	29.23	40.08	22.71	52.88
Liquid holdup					
ε_1 (%)	1.72	25.69	13.77	38.83	–56.22
ε_2 (%)	17.03	26.56	15.73	38.83	56.22
ε_3 (%)	124.09	98.75	69.28	120.32	87.87
ε_4 (–)	-1.2×10^{-3}	3.3×10^{-3}	1.7×10^{-3}	5.4×10^{-3}	-1.1×10^{-2}
ε_5 (–)	3.0×10^{-3}	3.6×10^{-3}	2.3×10^{-3}	5.4×10^{-3}	1.1×10^{-2}
ε_6 (–)	2.2×10^{-2}	1.1×10^{-2}	1.1×10^{-2}	8.9×10^{-3}	3.9×10^{-2}
$e_{Overall}$ (%)	612.34	266.55	213.19	324.93	298.79

Table 2—Statistical analysis of common model performance regarding liquid-holdup and pressure-gradient predictions.

version 2012 were also compared with the experimental three-phase-flow data of this study. The considered flow characteristics include liquid holdup, pressure gradient, wetted-wall fraction, and aqueous-phase fraction. **Figs. 19 and 20** show the comparison of available experimental data for three-phase flow with the mentioned predictive tools for pressure gradient and liquid holdup, respectively. The behaviors are similar to the two-phase-flow predictions for both models. Despite minor overprediction of liquid holdup and underprediction of pressure gradient, the predictions from the transient multiphase software are in acceptable agreement with experimental data. Predictions of the TUFFP unified model version 2012 are showing a more significant discrepancy. Three-phase-flow liquid-holdup and pressure-gradient data are both underpredicted by the model in a manner similar to the two-phase-flow case.

Fig. 21 shows the transient multiphase-simulation software and unified-model predictions for the flowing-aqueous-phase fraction in comparison with the acquired experimental data for three-phase flow. The results include all values of v_{SL}, v_{Sg}, and water cut. As observed earlier, the aqueous-phase fraction changes with gas-flow rate and approaches the inlet-stream fraction for higher v_{Sg} values, showing uniform mixing in the liquid phase. The predictions from the transient multiphase-simulation software apparently do not capture this behavior, and the predicted aqueous-phase-fraction values are almost constant for each of the given input values of water cut in the liquid phase (WC). No partial mixing of phases is predictable in the software, and the two liquid phases can be either separated or dispersed. For all the cases investigated in this study, the software predicted separated and wavy oil/aqueous-phase-flow regimes. This causes the discrepancy in aqueous-phase-fraction calculation for higher v_{Sg} cases in which the phases are more mixed. By use of the TUFFP unified model for all the three-phase cases of this study, the predicted liquid-phase-flow pattern is separated for v_{Sg} values less than 12.3 m/s and switches to dispersed flow pattern at greater than this value. The aqueous-phase fraction is underpredicted for most cases. However, the changing trends in aqueous-phase fraction are predicted better when compared with the results of the transient multiphase-simulation software. This can be attributed to a better estimate of transition from the separated- to the dispersed-flow pattern. However, the scatter in the data is still noticeable, showing some discrepancy between the predicted and experimental

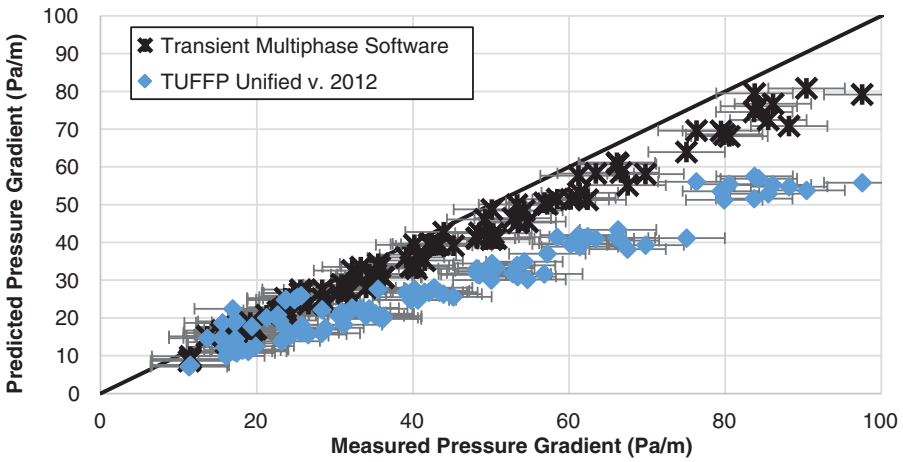

Fig. 19—Pressure-gradient data comparison with model predictions (three-phase flow).

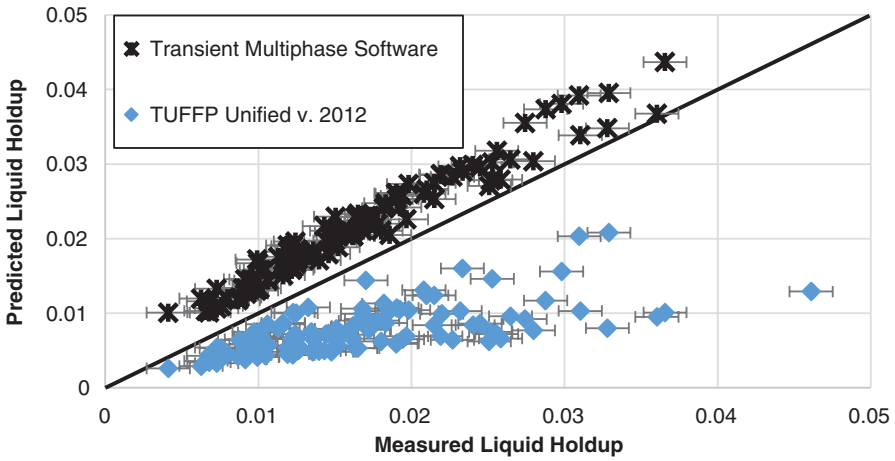

Fig. 20—Liquid-holdup data comparison with model predictions (three-phase flow).

values. This is probably because of an oversimplification of transition between the two liquid-phase-flow patterns.

Conclusions

An experimental study was conducted by use of a 6-in.-ID facility to investigate different characteristics of three-phase stratified wavy flow in horizontal pipelines. The experiments were conducted under low-liquid-loading condition, and the independently varied flow parameters were v_{Sg}, v_{SL}, and water-cut values.

The changes in the wave regime under stratified-flow pattern were observed. With increasing v_{Sg} values, the wave regime changed from stratified smooth to 2D waves, then to 3D waves, and finally to a roll-wave regime. The onset of droplet atomization occurred under the roll-wave regime. Moreover, with increasing v_{Sg} values, an increasing trend in pressure gradient and a decreasing trend in liquid holdup are observed, and the flowing *APF* approaches the inlet *WC,* showing a more-uniform liquid phase. The case of oil/air two-phase flow exhibits slightly lower liquid-holdup and higher pressure-gradient values in comparison to the cases with water in the liquid phase.

Predictions of Andritsos and Hanratty (1987) for the wave-pattern change and onset of entrainment are in acceptable agreement with the experimental data. The predictions of a transient multiphase-simulation software, the TUFFP unified model version 2012, Beggs and Brill (1973), Taitel and Dukler (1976), and Xiao et al. (1990) were compared with the acquired experimental data. The results from the transient multiphase-simulation software and the models of Taitel and Dukler (1976) and Xiao et al. (1990) are in better agreement with experimental liquid-holdup and pressure-gradient data, but the three-phase aqueous-phase-fraction predictions of the TUFFP unified model are in a better agreement with experimental data, compared to transient-multiphase-simulation-software predictions.

Nomenclature

APF = flowing aqueous-phase fraction
$DWWF$ = dynamic wetted-wall fraction
e_{Overall} = overall correlation discrepancy with experimental data, %
f_I = interfacial friction factor, dimensionless
H_L = liquid holdup, dimensionless
$H_{L,\max}$ = maximum liquid holdup in a given data set, dimensionless
PG = pressure gradient, Pa/m
$PG_{\max}$ = maximum pressure gradient in a given data set, Pa/m
v_{Sg} = gas-phase superficial velocity, m/s
$v_{Sg,\text{atom}}$ = onset of entrainment-gas-phase superficial velocity, m/s
v_{SL} = liquid-phase superficial velocity, m/s
WC = water cut in the liquid phase, dimensionless
ε_1 = average percent error, %
ε_2 = absolute average percent error, %
ε_3 = percent standard deviation, %
ε_4 = average error, dimensionless

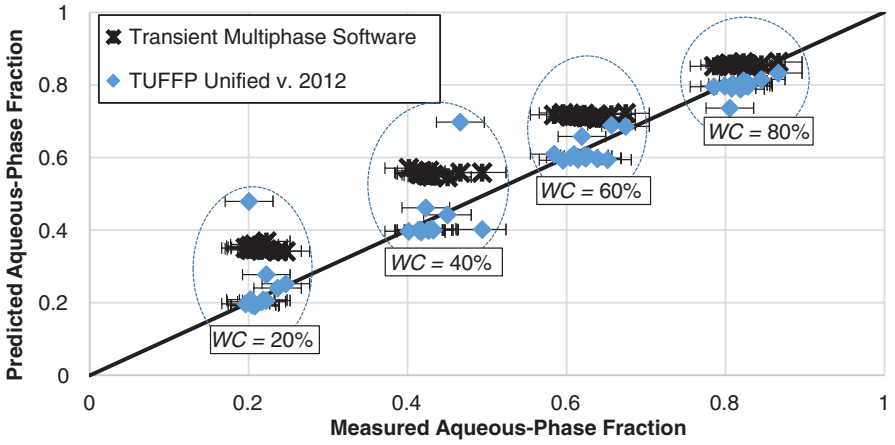

Fig. 21—Aqueous-phase-fraction data comparison with model predictions (three-phase flow).

ε_5 = absolute average error, dimensionless
ε_6 = standard deviation, dimensionless
μ = fluid viscosity, Pa·s
ρ = fluid density, kg/m^3
σ = liquid-phase surface tension, N/m

Acknowledgments

The authors thank the members of TUFFP for their support of this research.

References

Andritsos, N. and Hanratty, T. J. 1987. Influence of Interfacial Waves in Stratified Gas-Liquid Flows. *AIChE Journal* **33** (3): 444–454. http://dx.doi.org/10.1002/aic.690330310.

Beggs, D. H. and Brill, J. P. 1973. A Study of Two-Phase Flow in Inclined Pipes. *J Pet Technol* **25** (5): 607–617. SPE-4007-PA. http://dx.doi.org/10.2118/4007-PA.

Bendiksen, K. H., Maines, D., Moe, R. et al. 1991. The Dynamic Two-Fluid Model OLGA: Theory and Application. *SPE Prod Eng* **6** (2): 171–180. SPE-19451-PA. http://dx.doi.org/10.2118/19451-PA.

Dong, H. K. 2007. *Low Liquid Loading Gas-Oil-Water Flow in Horizontal Pipes*. MS thesis, The University of Tulsa, Tulsa, Oklahoma.

Fan, Y. 2005. *An Investigation of Low Liquid Loading Gas-Liquid Stratified Flow in Near-Horizontal Pipes*. Doctoral dissertation, The University of Tulsa, Tulsa, Oklahoma.

Gawas, K. 2013. *Studies in Low-Liquid Loading in Gas/Oil/Water Three Phase Flow in Horizontal and Near-Horizontal Pipes*. Doctoral dissertation, The University of Tulsa, Tulsa, Oklahoma.

Karami, H. 2015. *Three-Phase Low Liquid Loading Flow and Effects of MEG on Flow Behavior.* Doctoral dissertation, The University of Tulsa, Tulsa, Oklahoma.

Meng, W., Chen, X. T., Kouba, G. E. et al. 2001. Experimental Study of low-Liquid-Loading Gas-Liquid Flow in Near-Horizontal Pipes. *SPE Prod & Fac* **16** (4): 240–249. SPE-74687-PA. http://dx.doi.org/10.2118/74687-PA.

Taitel, Y. and Dukler, A. E. 1976. A Model for Predicting Flow Regime Transitions in Horizontal and Near Horizontal Gas-Liquid Flow. *AIChE Journal* **22** (1): 47–55. http://dx.doi.org/10.1002/aic.690220105.

Xiao, J. J., Shoham, O., and Brill, J. P. 1990. A Comprehensive Mechanistic Model for Two-Phase Flow in Pipelines. Presented at the SPE Annual Technical Conference and Exhibition, New Orleans, 23–26 September. SPE-20631-MS. http://dx.doi.org/10.2118/20631-MS.

Zhang, H. Q., Wang, Q., Sarica, C. et al. 2003. Unified Model for Gas-Liquid Pipe Flow via Slug Dynamics—Part 1: Model Development. *J. Energy Resour. Technol.* **125** (4): 266–273. http://dx.doi.org/10.1115/1.1615246.

Hamidreza Karami is a research associate at the McDougall School of Petroleum Engineering, working as a post-doctoral fellow with TUFFP and Horizontal Wells Artificial Lift Projects (TUHWALP) at the University of Tulsa. He also worked as a research assistant in the Paraffin Deposition Projects (TUPDP) and TUFFP. Karami's research interests are flow assurance, multiphase-flow dynamics, and production engineering. He holds a BS degree from Sharif University of Technology, Tehran, Iran, and MSc and PhD degrees from the University of Tulsa, all in petroleum engineering. Karami is a member of SPE.

Carlos F. Torres is a professor at the University of Los Andes, Venezuela. He has worked as a research associate with TUFFP and TUHWALP at the University of Tulsa, and also in the Chemical Engineering Department at University College London, UK. Torres' research interests are single-phase and multiphase flow, computational fluid dynamics, and mathematical modeling of energy systems. He holds a BS degree in mechanical engineering and an MS degree in applied mathematics, both from the University of Los Andes, Venezuela, and a PhD degree in mechanical engineering from the University of Tulsa.

Eduardo Pereyra is an assistant professor at the McDougall School of Petroleum Engineering and associate director of TUFFP and TUHWALP at the University of Tulsa. His research interests are multiphase-flow systems and transport, flow assurance, artificial lift, and separation technologies. Pereyra has published several refereed-journal and conference papers in his area of interest. He holds two BE degrees, one in mechanical engineering and one in system engineering, from the University of Los Andes, Venezuela, and MS and PhD degrees in petroleum engineering, both from the University of Tulsa.

Cem Sarica, F.H. "Mick" Merelli/Cimarex Energy Professor of Petroleum Engineering at the University of Tulsa, is currently serving as the director of three industry-supported consortia: TUFFP, TUPDP, and TUHWALP. His research interests are production engineering, multiphase flow in pipes, flow assurance, and horizontal wells. Sarica has authored or coauthored more than 150 publications. He holds BS and MS degrees in petroleum engineering from Istanbul Technical University and a PhD degree in petroleum engineering from the University of Tulsa. Sarica currently serves as a member of the SPE Projects, Facilities, and Construction Advisory Committee; second vice-chair of the SPE Flow Assurance Technical Section; and the chairperson-elect for the Projects, Facilities, and Construction Committee for the 2016 SPE Annual Technical Conference and Exhibition. He has previously served as a member of the SPE Production Operations Committee and the SPE Books Committee; chair of the SPE International Projects, Facilities, and Construction Award Committee and the Production & Operations Award Committee; and was a member of the *SPE Journal* editorial board between 1999 and 2007. Sarica is the recipient of the 2010 SPE International Production and Operations Award, and was recognized as a Distinguished Member of SPE in 2012. He received the SPE John Franklin Carll Award and the SPE Cedric K. Ferguson Certificate in 2015.